AIAA 81-0016R

Numerical Optimization of Circulation Control Airfoils

Tsze C. Tai*
David Taylor Naval Ship Research and Development Center, Bethesda, Md.
George H. Kidwell Jr.†
NASA Ames Research Center, Moffett Field, Calif.
and
Garret N. Vanderplaats‡
Naval Postgraduate School, Monterey, Calif.

A numerical procedure for optimizing circulation control airfoils, which consists of the coupling of an optimization scheme with a viscous-potential flow analysis for blowing jet, is presented. Without losing the generality of the methodology, special attention is given to optimizing the blunt trailing edge, which has a direct bearing on the jet deflection characteristics. The desired airfoil is defined by a combination of three baseline shapes: cambered ellipse, cambered ellipse with drooped trailing edge, and cambered ellipse with spiraled trailing edge. The coefficients of these shapes are used as design variables in the optimization process. Under the constraints of lift augmentation and lift-to-drag ratios, the optimal airfoils are found to lie between those of the cambered ellipse and the drooped trailing edge, toward the latter as the angle of attack increases. Results agree qualitatively with the available experimental data.

Nomenclature

a_j = airfoil coefficients (used as design variables)
C_c = chordwise force coefficient
C_D = drag coefficient (total)
C_L = lift coefficient
C_n = normal force coefficient
C_p = pressure coefficient
C_μ = blowing momentum coefficient
c = chord length
M = Mach number
N = number of panels
q = source strength
S = direction of search in the n-dimensional design space
s = arc length along airfoil surface
t = thickness
V = velocity
x,y = airfoil coordinates
α = angle of attack
α^* = scalar defining distance of travel
Γ = total circulation
δ^* = boundary layer displacement thickness

Subscripts

e = edge of boundary layer
f = frictional
i = ith panel
p = pressure
sepl = separation point, lower surface
sepu = separation point, upper surface
∞ = freestream

Presented as Paper 81-0016 at the AIAA 19th Aerospace Sciences Meeting, St. Louis, Mo., Jan. 12-15, 1981; submitted Feb. 19, 1981; revision received July 1, 1981. This paper is declared a work of the U.S. Government and therefore is in the public domain.

*Research Aerospace Engineer, Aviation and Surface Effects Department. Member AIAA.
†Research Aerospace Engineer, Helicopter and Powered Lift System Division. Member AIAA.
‡Associate Professor, Department of Mechanical Engineering. Member AIAA.

Introduction

IN the development of technology for V/STOL aircraft, efforts have been made to increase the lift coefficient through blowing. Systems that use blowing may be classified into three major categories: 1) blowing flap, 2) jet flap, and 3) circulation control airfoils. In the application of blowing to helicopter rotors, the circulation control (CC) system offers two basic advantages; namely, the much higher lift-to-thrust augmentation for a given slot momentum and the mechanical simplifications in lift control.

Experimental data are available for circulation control airfoils.[1-4] The analytical method developed earlier on a circular cylinder used an integral approach to model the flow as an incompressible turbulent boundary layer flow mixed with a wall jet.[5] Later, Dvorak and Kind solved the wall jet flow over elliptical airfoils by a finite difference scheme but retained the integral approach for flow regions where ordinary boundary layers prevail.[6] Reasonably good lift-momentum results have been reported using these methods, although a major deficiency in drag prediction still exists. Attempts to incorporate a more realistic eddy viscosity model have been reported by Wood.[7]

To meet the performance requirement for several naval applications, an optimization procedure is highly desirable to provide an advanced design capability. In the present work, a numerical approach is taken to optimize the airfoil for maximum lift. Various constraints including thickness, lift-to-drag ratio, and lift-momentum flux relations are imposed to generate optimal airfoil shapes. In so doing, a numerical optimization scheme of Vanderplaats[8] for linear or nonlinear constrained problems has been employed and coupled with a viscous-potential flow interaction analysis of Dvorak and Kind[6] for necessary viscous-inviscid flowfield calculations. Reasonably good agreement between theoretical and experimental results for certain cases has been reported to warrant some confidence in the method.

Analysis Method

A schematic of the flow about a CC airfoil is shown in Fig. 1. As opposed to the conventional airfoil, a typical CC airfoil is equipped with a blowing slot on the upper surface for energizing the flow in the viscous layer and a rounded trailing

edge for deflecting the jet. High lift can be generated because of increased circulation created by the blowing jet. The flow is characterized by outer inviscid flow and inner viscous flow consisting of boundary layers, wall jet, and separation bubble.

Rather than starting from scratch, the analysis method developed by Dvorak and Kind[6] was adopted with some minor modifications. The method is the most comprehensive available. Dvorak and Kind[6] considered the subject problem as a viscous-potential flow interaction over a two-dimensional airfoil section with or without slot blowing on the upper surface. The incompressible potential flow is calculated by vorticity distribution along the panels. The vortex strength is assumed to vary linearly along each panel and is continuous at all junction points. The solution procedure is similar to those for conventional airfoils except that the Kutta condition is applied differently. For a rounded trailing edge, which is typical in a CC airfoil, the Kutta condition is satisfied by specifying the value of the total circulation around the airfoil.

The forward and aft stagnation points obtained by the potential flow solution divide the flows between the upper and lower surfaces of the airfoil. Based on pressures obtained from the potential flow solution, calculation of boundary layers starts with the Hiemenz stagnation flow solution.[9] Curle's integral method[10] is employed for calculating the laminar boundary layers downstream of the stagnation point for both upper and lower surfaces. After the transition predicted by Granville's empirical formula,[11] the turbulent boundary layers for the remaining lower surface to the separation point, and the upper surface to the blowing slot are calculated using the Nash-Hicks integral method.[12] At the slot, the turbulent boundary layer mixes with a wall jet of known velocity distribution (essentially uniform). A finite difference scheme of the Crank-Nicolson type is used in solving the mixed flow. The flow proceeds around a highly curved surface with very strong adverse pressure gradients. The effect of the surface curvature downstream of the blowing slot is accounted for by including the curvature terms in the streamwise momentum equation, and adding the normal momentum equation for radial variation of static pressure in the finite difference procedure. The flow eventually separates after passing the blunted trailing edge, and a separation pressure is noted.

The viscous effects produced by the boundary layer development are modeled by a source distribution along the airfoil surface. The source strength q_i at any junction point of a surface panel is obtained by

$$q_i = \frac{\mathrm{d}}{\mathrm{d}s}(V_e \delta^*) \tag{1}$$

Equation (1) applies to the conventional boundary layers as well as to the wall jet. In the latter case, the product $V_e\delta^*$ tends to decrease, yielding a negative source strength (i.e., sink).

The contribution of q_i is then implemented in the potential flow solution, which alters the results of the pressure distribution. The entire procedure is then repeated with subsequent values of the total circulation estimated by

$$\Gamma_{m+1} = \Gamma_m + k(C_{p_{\text{sepu}}} - C_{p_{\text{sepl}}}) \tag{2}$$

where the numerical constant k has a value of from 0.1 to 0.3. The calculations are terminated when the lift coefficient (directly related to the Γ_{m+1} value) remains within a specified tolerance and, at the same time, the differences in pressure coefficients at the upper and lower ends of the separation bubble diminish. The lift and pressure drag coefficients are then evaluated by integrating the surface pressure distribution using the trapezoidal rule.

The method has been coded and known as the CIRCON program. It has been written in an overlay form to reduce core requirements. A detailed description of the code is given by Dvorak.[13]

A major difficulty in using the viscous-inviscid interaction method with the optimization code, however, is its inability in providing fairly smooth gradients of the objective function when the design variables are perturbed in the course of optimization. The problem is common in most viscous-inviscid interaction methods where the viscous and inviscid flows are calculated separately, and the final solution is reached by the iterative process. To smooth out some irregularities of the iteratively determined pressure distribution, a second-order Lagrangian interpolation scheme is adopted for integrating the force coefficients:

$$C_n = \sum_{i=1}^{N+1} \left[C_{p_i}\left(\frac{x_{i+1}-x_{i-1}}{x_i - x_{i-1}} + 2\right) + C_{p_{i+1}}\left(\frac{x_i - x_{i-1}}{x_{i+1}-x_{i-1}} + 2\right) - C_{p_{i-1}}\left(\frac{(x_{i+1}-x_i)^2}{(x_i - x_{i-1})(x_{i+1}-x_{i-1})}\right)\right] \frac{(x_{i+1}-x_i)}{6} \tag{3}$$

For evaluating C_c, x's are replaced by y's.

The use of the Lagrangian scheme has improved the convergences of C_L values to a certain extent, as discussed in Ref. 14. However, it has little effect on the accuracy of calculated C_L values, which is dominated by the panel arrangement rather than by any smoothing device.

It is noted that for CC airfoils, the total drag coefficient is the sum of the pressure drag and skin friction, less the blowing momentum coefficients

$$C_D = C_{D_p} + C_{D_f} - C_\mu \tag{4}$$

where the blowing momentum coefficient is defined by

$$C_\mu \equiv 2\rho_j V_j^2 h / \rho_\infty V_\infty^2 c \tag{5}$$

The symbol $\rho_j V_j^2$ is the momentum flux of the blowing jet, and h is the jet height at the slot. Among the three, the pressure drag is the dominating component of the total drag. Fluctuations in pressure coefficient, resulting from alternating viscous-inviscid calculations, directly pass on to the total drag. The magnitude of the fluctuations far exceeds the remedy of the smoothing effort that an integration scheme can provide. Consequently, the calculated drag values exhibit serious deficiencies in comparison with experimental data.

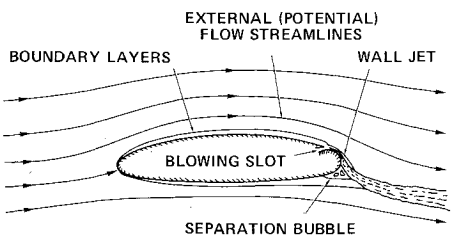

Fig. 1 Flow around a circulation control airfoil.

Optimization Procedure

Optimization Model

The subject problem is to optimize the airfoil for maximum lift, minimum drag, or maximum lift-to-drag ratio. Various constraints, including minimum lift range, maximum drag range, angle of attack, lift augmentation ratio, thickness ratio, jet detachment, and linear lift-momentum flux relations, can be imposed to generate optimal airfoil shapes. The problem is best handled by a numerical optimization scheme developed by Vanderplaats.[8]

The optimization model for the problem contains the objective, the constraints, and the design variables. Because of the limited capability of the analysis method (i.e., deficiencies in calculated drag values), the present procedure is restricted to cases for maximizing the lift only. Therefore, for a typical case that optimizes the airfoil for maximum lift subject to thickness ratio and lift-to-drag constraints, the optimization model would be

1) minimize objective:

$$-C_L(X)$$

2) constraints:

$$(t/c)_{\min} \le t/c \le (t/c)_{\max} \tag{6}$$

$$(C_L/C_D)_{\min} \le C_L/C_D \le (C_L/C_D)_{\max} \tag{7}$$

3) design variables—X:a_j, $j=1, n$

where a_j is the coefficient in the equation that represents the airfoil shape to be optimized. The lift coefficient C_L and the drag coefficient C_D are nonlinear implicit functions of the design variables to be obtained by the analysis methods, and the thickness ratio is a linear function of the design variables.

The optimization program begins with an initial X vector which is input to the program and may or may not define a feasible design. The optimization process then proceeds iteratively by the following recursive relationship:

$$X^{m+1} = X + \alpha^* S^m \tag{8}$$

The S^m is obtained by moving in the direction of the steepest descent (the negative gradient of the objective function) without violating constraints. The scalar α^* is determined by a one-variable search based on a polynomial fit of several trial values. The procedure is repeated with the aid of a conjugate direction algorithm[15] in determining the new search direction. When the constraint is encountered in the searching process, the new search direction is found using Zoutendijk's method of feasible directions.[16] The optimum point is achieved where no direction can be found that will reduce the objective without violating the constraints.

Airfoil Representation and Panel Arrangement

Airfoil Representation

To facilitate the optimization process, the design airfoil is represented by a linear combination of n baseline profiles:

$$Y = \sum_{j=1}^{n} a_j Y_j \tag{9}$$

where Y_j represents the coordinates of fixed baseline profile. Perturbation in coefficients a_j directly leads to changes of the resulting airfoil shape. Therefore a_j's constitute effective design variables. While the airfoil equation, Eq. (9), is general for overall airfoil shaping, the first effort is to contour the blunt trailing edge because of its direct bearing on the jet deflection characteristics. Three baseline shapes, i.e., a cambered ellipse, a cambered ellipse with a drooped trailing edge, and a cambered ellipse with a logarithmically spiraled trailing edge, are employed in test cases. These shapes (shown in Fig. 2) are considered representative of airfoils suitable for circulation control purposes. Equation (9), therefore, simplifies to

$$Y = a_1 Y_1 + a_2 Y_2 + a_3 Y_3 \tag{10}$$

The exact coordinates of these baseline airfoils are given in Ref. 14.

All three baseline shapes have identical coordinates up to $x/c=0.95$. Variation is allowed between $0.95 \le x/c \le 1.00$. For this special case, because the thickness of the resulting airfoil remains constant, there yields

$$a_1 + a_2 + a_3 = 1 \tag{11}$$

Accordingly, Eq. (10) can be written as

$$Y = a_1 Y_1 + a_2 Y_2 + (1 - a_1 - a_2) Y_3 \tag{12}$$

The new form reduces the actual number of design variables from three to two, still with three baseline shapes. It, in turn, reduces the number of gradients and thus simplifies the search process. It also eliminates the thickness constraint, which is automatically satisfied. Note that because negative values of a_1, a_2, or a_3 are allowed, the resulting airfoil shape can be drastically different from those original profiles.

The ultimate purpose of the present work is to derive a CC airfoil for optimum performance. The work involves overall airfoil shaping based on more general representation of baseline profiles. The computer program has been set up to accept as many as 25 baseline shapes, although practically, 6 would be sufficient to cover a broad range of interest.

Panel Arrangement

Because of the large number of iterations involved in the optimization process, the number of panels associated with

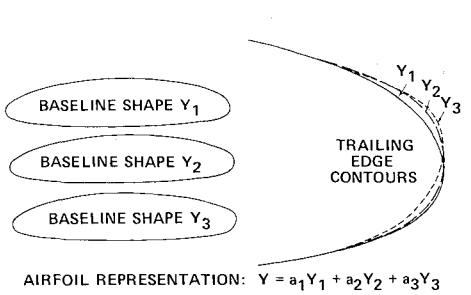

Fig. 2 Three baseline shapes for airfoil representation.

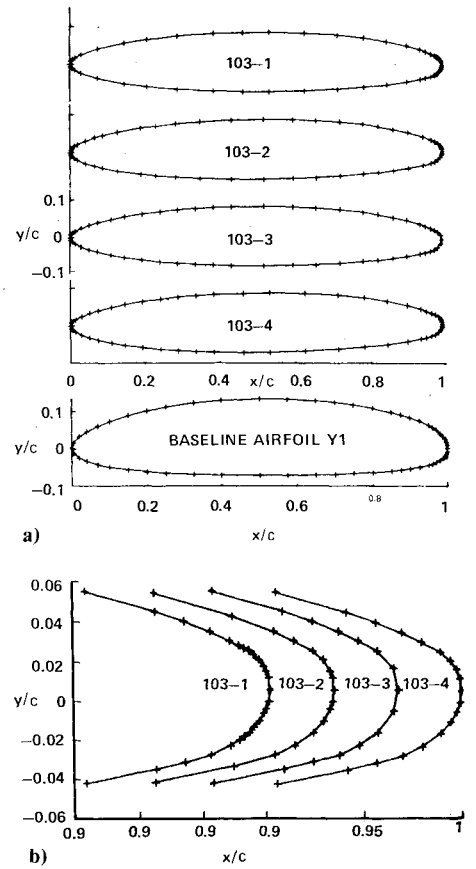

Fig. 3 Various panel arrangements of circulation control airfoils. a) Overall view; b) trailing edge detail.

the vortex distribution in the potential flow calculation must be kept low enough to conserve computer time, yet high enough to achieve reasonable accuracy. As a compromise, a total of 58 panels are used. Using the same spacing in the x coordinate, each surface of the airfoil has 29 panels. Special attention is then given to proper arrangement with this limited number of panels. As a general rule, relatively dense distribution in the trailing edge is required for detailed flow computations of the jet-boundary layer mixing region. On the other hand, too sparse a panel distribution in other regions might lead to unrealistic results.

To evaluate the effect of the panel arrangement on the lift coefficient values, a comprehensive study was conducted. The calculated results are compared with the available experimental data for the case of the CC airfoil model 103 at $M_\infty = 0.3$ and $\alpha = -0.01$ degree. Several arrangements were investigated; four are depicted in Fig. 3. For virtually the same airfoil with the same set of flow conditions, the resulting C_L can deviate significantly from one panel arrangement to the other, as indicated in Fig. 4. It is noted that the experimental data, which were taken from the DTNSRDC 7×10-ft transonic wind tunnel, can be bracketed with the results of the 103-1 and 103-3 arrangements. Arrangements 103-2 and 103-4 seem to yield C_L values that correlate fairly well with the experimental trend. Spacings that are similar to arrangement 103-4, therefore, were employed in all the optimization calculations; see Fig. 3a.

This study supersedes a spot-check-type evaluation of the analysis method (CIRCON) previously performed that appears in the section on "Comparison Between Theory and Experiment" in Ref. 14. The results of that evaluation were computed based on a different panel arrangement before a series of optimization runs, and therefore bear no effect on subsequent optimization calculations.

Computer Program

The optimization model is implemented numerically by interaction between the optimization code and the airfoil analysis method. The flow chart for such an operation is shown in Fig. 5. In so doing, the airfoil analysis program CIRCON, along with an airfoil representation routine, is combined with the optimization code CONMIN/COPES.§

The program can now perform optimization runs for maximizing the lift without substantial difficulty; but for minimizing the drag, further improvement of the analysis method is required. The program takes approximately 200,000 CM storage and 45 s on a CDC 7600 computer to perform one analysis calculation, with ten iterations between the potential and viscous flows. A typical optimization run requires about 15 to 20 calls on the analysis program, which amounts to 10 to 15 min on a CDC 7600 computer.

Results and Discussion

Numerical results were calculated on the NASA Ames CDC 7600 computer using a remote terminal at DTNSRDC. The integrated program was first checked by the ANALYSIS, SENSITIVITY STUDY, and TWO-VARIABLE SPACE modes in accordance with the control options of the main program COPES before extensive OPTIMIZATION mode runs were performed. Results of the ANALYSIS runs are discussed in the previous section. A more detailed presentation can be found in Ref. 14.

The first optimization run was a simple case for minimizing the frictional drag with the angle of attack as the design variable. The results of this run yield a slight decrease in skin friction corresponding to a change of the design variable α from -5 to -4.9 deg. The purpose of the run was to test the status of the program rather than to actually design for minimum skin friction, which is just a small portion of the total drag and has only a small range of variation.

Subsequent efforts were concentrated on cases using the lift coefficient as the objective. Numerical results were obtained for maximizing C_L with a blowing momentum coefficient C_μ of 0.04, at a Mach number of 0.3, and at angles of attack of -5 and -2 deg. Constraints of the lift augmentation ratio, $50 \le C_L/C_\mu \le 60$, and the drag-to-lift ratio, $-0.014 \le C_D/C_L \le -0.006$, were imposed. Figure 6 shows the values of C_L vs the search position during the course of optimization for the case of $\alpha = -5$ deg. The search starts with $a_1 = 0.3333$ and $a_2 = 0.3334$, which yields $C_L = 2.054$. The search stops after the change of the objective function within a specified tolerance, consecutively for three times. A final lift coefficient of 2.34, is achieved with design variables $a_1 = 0.4084$, $a_2 = 0.4798$, and $a_3 = 0.1180$. A similar run with less restrictive

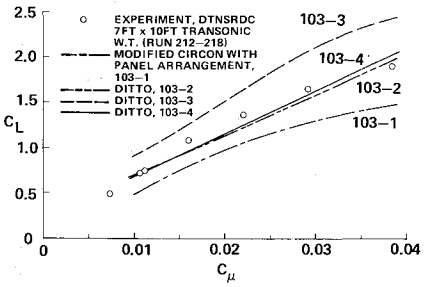

Fig. 4 Effect of panel arrangement on lift coefficient of model 103 at $M_\infty = 0.3$ and $\alpha = -0.01$ deg.

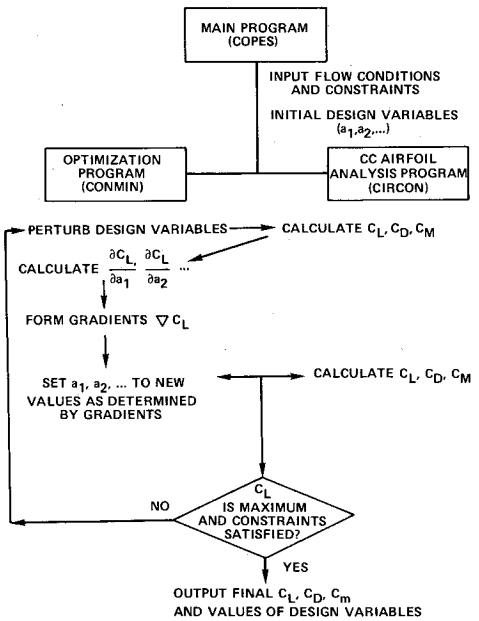

Fig. 5 Program flow chart.

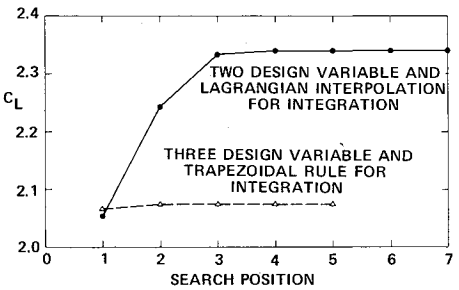

Fig. 6 Lift coefficient during the course of optimization at $M_\infty = 0.3$, $C_\mu = 0.04$, and $\alpha = -5$ deg.

§A control program called COPES has been added to the CONMIN by Vanderplaats.

constraints, but using three design variables along with the original trapezoidal rule integration, is also plotted in Fig. 6. Results indicate that the advantage of using the recast airfoil equations along with the Lagrangian scheme is distinctive.

Figure 7 shows the C_L values in the two-variable design space. Continuity of C_L values in most regions is maintained, as marked by solid lines. Some uncertainty is involved in the region with broken lines. As a double check, the intermediate C_L values of Fig. 6 are superimposed in Fig. 7. The optimal value approaches the true maximum fairly closely. The C_L value tends toward, but terminates before, the maximum because the termination criterion has been met. The test warrants further inclusion of more baseline shapes in representing the airfoil so that greater versatility may be achieved.

The resulting airfoil profile, shown in Fig. 8, is somewhat between baseline shapes Y_1 and Y_2. The results agree qualitatively with the available experimental data for which the airfoils having cambered ellipse and drooped trailing edge contours exhibit better performance than does the spiraled one. It is of interest to note that at negative angles of attack where the CC airfoils normally operate, high C_L values are usually accompanied by low drag coefficient.

Figure 9 shows C_L values during the optimization process for the case of $M_\infty = 0.3$, $C_\mu = 0.04$, and $\alpha = -2$ deg. The calculation was terminated after five searches: the C_L values gained from 2.255 to 2.740. The final design ended with $a_1 = 0.499$, $a_2 = 0.624$, and $a_3 = -0.123$. The resulting airfoil is depicted in Fig. 10. Note that a_3 has a negative value, which yields a more drooped trailing edge than the previous case of $\alpha = -5$ deg.

Finally, the effect of the constraint on the resulting C_L values is examined. This is shown in Fig. 9, where the results with constraints encountered during the course of optimization are compared with those without constraints encountered. Considerable penalty due to the active constraints are realized.

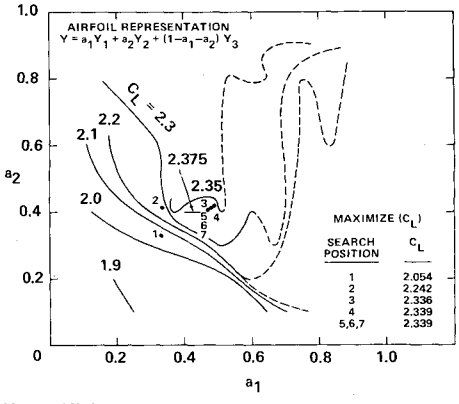

Fig. 7 Lift coefficients in two-variable space at $M_\infty = 0.3$, $C_\mu = 0.04$, and $\alpha = -5$ deg.

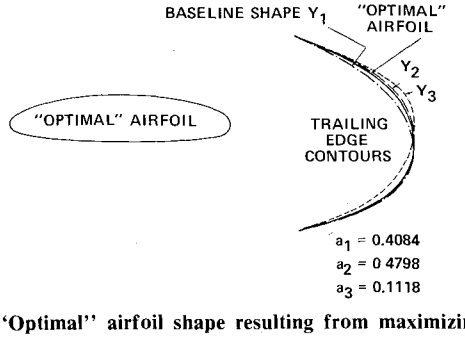

Fig. 8 "Optimal" airfoil shape resulting from maximizing C_L at $M_\infty = 0.3$, $C_\mu = 0.04$, and $\alpha = -5$ deg.

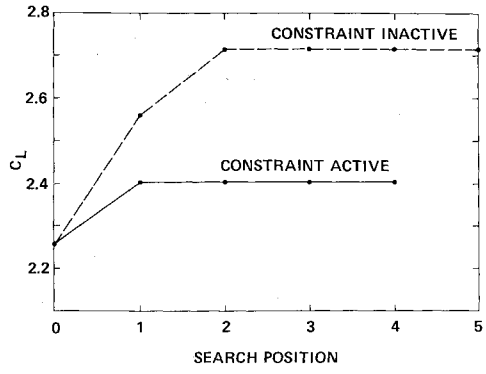

Fig. 9 Effect of constraint in optimization.

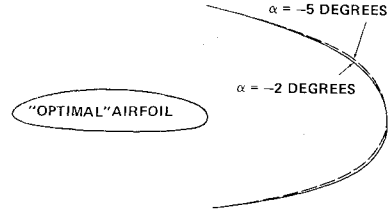

Fig. 10 "Optimal" airfoil shape resulting from maximizing C_L at $M_\infty = 0.3$, $C_\mu = 0.04$, and $\alpha = -2$ deg.

Conclusions

A numerical procedure for optimizing circulation control airfoils is developed. Based on the first phase of work in the continuing effort of improving aerodynamic performance of the CC airfoil, the following conclusions may be drawn:

1) A significant gain (about 12 to 15%) in lift coefficients of CC airfoils may be achieved by optimizing the trailing edge contour. In the range of small negative angles of attack, the drooped trailing edge yields better aerodynamic performance than does the spiraled one.

2) A major difficulty in using the viscous-inviscid interaction method along with the optimization code is its inability to provide fairly smooth gradients of the objective function. It is possible, however, to make optimum calculations for maximum lift by reducing the number of design variables to the minimum and removing some irregularities in integrating aerodynamic force coefficients from the surface pressure distribution. For minimizing the drag, further improvement of the analysis method is required.

3) Panel spacing has a direct effect on the results. Care must be exercised to ensure proper panel arrangement that will produce results to yield reasonable correlation with the experimental trend.

Acknowledgments

This work was supported by the Independent Research Program at DTNSRDC under work unit 1606-105. The NASA Ames Research Center has provided computer support. The authors acknowledge the assistance of E.O. Rogers, J.S. Abramson, and J.B. Wilkerson, and the enlightening discussions with R.M. Williams, S. de los Santos, and D.A. Jewell, all of the David Taylor Naval Ship Research and Development Center.

References

[1] Cheeseman, I.C. and Seed, A.R. "The Application of Circulation Control by Blowing to Helicopter Rotors," *The Aeronautical Journal*, Vol. 71, No. 679, July 1967, pp. 451-467.

[2] Williams, R.M. and Rogers, E.O., "Design Considerations of Circulation Controlled Rotors," 28th Annual Forum of American Helicopter Society, AMC Paper 603, Washington, D.C., May 1972.

[3] Walters, R. E., Myer, D.P., and Daniel, J., "Circulation Control by Steady and Pulsed Blowing for a Cambered Elliptical Airfoil,"

Aerospace Engineering Rept. TR-32, West Virginia University, Morgantown, W.Va., July 1972.

[4]Englar, R.J., "Two-Dimensional Transonic Wind Tunnel Tests of Three 15% Thick Circulation Control Airfoils," NSRDC ASED Rept. 182, Dec. 1970.

[5]Levinsky, E.S. and Yeh, T.T., "Analytical and Experimental Investigation of Circulation Control by Means of a Turbulent Coanda Jet," NASA CR-2114, Sept. 1972.

[6]Dvorak, F.A. and Kind, R.J., "Analysis Method for Viscous Flow Over Circulation-Controlled Airfoils," *Journal of Aircraft,* Vol. 16, Jan. 1979, pp. 23-28.

[7]Wood, N.J., "The Aerodynamics of Circulation Controlled Aerofoils—A Progress Report," University of Bath, School of Engineering, England, Rept. 439, Jan. 1978.

[8]Vanderplaats, G.N., "CONMIN—a FORTRAN Program for Constrained Function Minimization," NASA TM X-62282, Aug. 1973.

[9]Schlichting, H., *Boundary Layer Theory,* 4th Ed., McGraw-Hill, New York, 1960, pp. 147-151.

[10]Curle, H., "A Two-Parameter Method for Calculating the Two-Dimensional Incompressible Laminar Boundary Layer," *The Aeronautical Journal,* Vol. 71, Feb. 1967, pp. 117-123.

[11]Granville, P.S., "The Calculation of Viscous Drag of Bodies of Revolution," DTMB Rept. 849, 1953.

[12]Nash, J.F. and Hicks, J.G., "An Integrated Method Including the Effect of Upstream History on the Turbulent Shear Stress," *Proceedings of Computation of Turbulent Boundary Layer,* AFOSR-1FP-Stanford Conference, Vol. 1, 1968, pp. 37-45.

[13]Dvorak, F.A., "A Computer Program for the Viscous/Potential Flow Interaction Analysis of Circulation Controlled Airfoils," Analytical Methods Rept. 75-01, Bellevue, Wash., April 1975.

[14]Tai, T.C., Kidwell, G.H. Jr., and Vanderplaats, G.N., "Numerical Optimization of Circulation Control Airfoils," DTN-SRDC Rept. 80/060, April 1980.

[15]Fletcher, R. and Reeves, C.M., "Function Minimization by Conjugate Directions," *British Computer Journal,* Vol. 7, No. 2, 1964, pp. 149-154.

[16]Zoutendijk, G.G., *Methods of Feasible Directions,* Elsevier, Amsterdam, 1960.